Journal of Inorganic and General Chemistry
ZAAC
Zeitschrift für anorganische und allgemeine Chemie
www.zaac.wiley-vch.de
RESEARCH ARTICLE

DOI: 10.1002/zaac.202200201

Characterization of the Binary Nitrides VN and ScN by Solid-State NMR Spectroscopy

Jennifer Steinadler,[a] Lucien Eisenburger,[a] and Thomas Bräuniger*[a]

Dedicated to Professor Wolfgang Schnick on the Occasion of his 65th Birthday

NMR spectra of polycrystalline samples of the binary nitrides ScN and VN were acquired under magic-angle spinning. The observed nuclides ^{45}Sc, ^{51}V and ^{14}N are all quadrupolar nuclei with a spin $I > 1/2$. However, due to the high symmetry of their rock-salt type structures, the spectra of the nitrides do not exhibit effects of quadrupolar or other anisotropic interactions of significant magnitude. This allows a relatively straightforward evaluation of the acquired spectra, leading to isotropic chemical shift values (δ_{iso}) of -213 ppm (^{51}VN), 378 ppm (V^{14}N), 290 ppm (^{45}ScN) and 442 ppm (Sc^{14}N) against commonly used reference standards. In the wider context of ^{14}N-NMR of binary nitrides, it is shown that the distance of nitrogen to the nearest neighbour cation can be correlated to the observed chemical shift.

Introduction

Despite its challenging technical fixation, nitrogen is one of the most important elements for industrial processes. Nitrogen-containing compounds cover a wide range of applications, which is apparent already for members of the compound class with the simplest compositions, i.e. binary nitrides. For example, the wide-bandgap semiconductor aluminium nitride (AlN) with its high thermal conductivity and piezoelectric properties is a promising and widely used material not only for ultraviolet light-emitting diodes[1] but also in microelectromechanical systems (MEMS)[2] or tactile sensors.[3] Boron nitride occurs in both a cubic and a hexagonal modification. With its special properties, *c*-BN is a useful material for cutting devices used in the machining process of ferrous alloys to avoid graphitization of diamond.[4] On the other hand, the 2D-layered *h*-BN is an excellent lubricant offering thermal and chemical stability which can be used in both a wide temperature and pressure range, and is also a good dielectric material.[5,6]

Binary nitrides of transition metals have also been synthesized, including titanium, vanadium as well as scandium nitride, all crystallizing in the rock-salt structure type. TiN is used to improve surface properties by coating,[7,8] and has also applications in microelectronics.[9] Likewise, VN possesses good electrical conductivity as well as a large electrochemical potential window which enables its use as anode material in supercapacitors[10] or as diffusion barrier.[11] ScN offers semi-conducting properties as well as a high thermal and mechanical stability. It is of interest for thermoelectrics[12] or as a compatible metal gate for n-type metal-oxide-semiconductors.[13]

Another important area of application is the use of binary nitrides as starting materials for synthesis. Aluminium nitride is a precursor in the production of SiAlON ceramics.[14] Titanium nitride has been reacted to obtain a range of target compounds, such as an oxonitridophosphate,[15] TiP_4N_8 polymorphs,[16] and both titanium pernitride[17] and cubic phase Ti_3N_4 under extreme pressure conditions.[18] Scandium nitride has long been considered mostly inert, but has recently been utilized for the synthesis of an oxonitridophosphate.[15] Due to the refractory character[19] of TiN and ScN, it has been necessary to activate these compounds under both high-pressure and high-temperature conditions, using NH_4F as mineralizing agent and HF source.[15,16] Obviously, it is of vital importance to monitor synthetic procedures by appropriate analytics. X-ray diffraction (XRD) methods are very powerful, but may fail to detect minority phases in powder samples due to their grains being too small or non-crystalline. Because of its capability of probing the local electronic surrounding of the investigated nuclei, solid-state NMR spectroscopy is a useful complementary technique for the characterization of inorganic solids.[20,21] In particular, it may be possible to trace otherwise undetected starting material in the products by NMR, as has been demonstrated for AlN in the synthesis of SiAlON compounds.[22,23]

In this work, we describe the NMR characterization of ^{45}Sc^{14}N and ^{51}V^{14}N, which may prove helpful for identifying these binary nitrides also in multi-phase systems.

---

[a] J. Steinadler, L. Eisenburger, Dr. T. Bräuniger
Department of Chemistry
University of Munich (LMU)
Butenandtstraße 5-13
81377 Munich, Germany
E-mail: Thomas.braeuniger@cup.lmu.de

Results and Discussion

Surveying the distribution of nuclides in the investigated nitrides, it can be concluded that the compounds may be denoted by $^{45}Sc^{14}N$ and $^{51}V^{14}N$ in very good approximation, with ^{45}Sc occurring with 100%, ^{51}V with 99.76% and ^{14}N with 99.63% natural abundance. This leads to obvious choices for NMR measurements. All nuclides considered here have a spin $I > 1/2$, and thus possess a quadrupolar moment.[24] The interaction of these quadrupolar moments with the electric field gradient (EFG) of the surroundings leads to additional terms in the NMR Hamiltonians, which are usually taken into account as perturbations of the Zeeman interaction. If the Larmor frequency is denoted by ν_0, and the chemical shift contribution by ν_{CS}, the resonance frequency $\nu(k)$ of a transition k may be written as:

$$\nu(k) = \nu_0 + \nu_{CS} + \nu_Q^{(1)}(k) + \nu_Q^{(2)}(k^2) + \ \dots \qquad (1)$$

For compact notation, we have used the parameter k to indicate the transitions, which is related to the familiar magnetic quantum number m by the relation $k = m \pm 1/2$ for the transition $m \rightarrow m \ \pm 1$.[25] Both ^{45}Sc and ^{51}V happen to possess spin $I = 7/2$, and their respective NMR spectra are composed of a central transition with $k = 0$, and three pairwise satellite transitions with $k = \pm 1, \pm 2, \pm 3$. In contrast, ^{14}N has $I = 1$, with only two possible transitions with $k = \pm 1/2$. The frequencies $\nu_Q^{(1)}$ and $\nu_Q^{(2)}$ in Equation (1) describe the contributions of the quadrupolar interaction to first and second order. Because of the high symmetry of the rock-salt structure type of the investigated nitrides, which leads to a highly symmetric EFG tensor, quadrupolar coupling should be completely absent in these compounds. As we will see below, the experimental spectra of ^{45}Sc and ^{51}V indicate the possible presence of some residual coupling, which can be adequately described using first-order contributions only.

Dipolar couplings between the magnetic moments of the nuclear spins are also present in our binary nitrides with high abundance. In principle, these constitute another term ν_{IS} in Equation (1). The coupling between two different spins I and S scales according to the equation (which includes the gyromagnetic ratios γ of the spins, and their distance r_{IS}):[26]

$$\nu_{IS}(\beta_{IS}) = \frac{\mu_0}{8\pi^2} \cdot \frac{\gamma_I \gamma_S \hbar}{r_{IS}^3} \cdot \frac{(3\cos^2\beta_{IS} - 1)}{2} = D_{IS} \cdot \frac{(3\cos^2\beta_{IS} - 1)}{2} \qquad (2)$$

Here, β_{IS} is the angle of the internuclear vector with the magnetic field, and D_{IS}, the dipolar coupling constant, constitutes a convenient measure of the interaction strength. In the binary nitrides under investigation here, the largest couplings experienced for the various observed nuclides are characterized by the following values for D_{IS}, which were calculated from the shortest distances taken from the XRD structure determinations: 219 Hz for ^{45}Sc–^{45}Sc spin pairs, 184 Hz for ^{45}Sc–^{14}N, 333 Hz for ^{51}V–^{51}V, and 259 Hz for ^{51}V–^{14}N (for homonuclear couplings, Equation (2) needs to be multiplied by a factor of 3/2 to obtain the maximum values). All spectra in this work, however, have been measured under magic-angle spinning (MAS), which reduces all contributions scaling with the term $(3\cos^2\beta_{IS} - 1)/2$.[27] With an applied MAS rate of 10 kHz, the dipolar couplings present in $^{45}Sc^{14}N$ and $^{51}V^{14}N$ are sufficiently small to be fully averaged out by MAS, justifying the omission of the term ν_{IS} in Equation (1).

NMR of spin-7/2: ^{45}Sc and ^{51}V

The MAS-spectra of ^{51}V and ^{45}Sc, both with spin $I = 7/2$, are shown in Figure 1 with single, strong resonances located at −213 ppm for vanadium nitride and 290 ppm in the case of scandium nitride. The high-intensity resonances can be identified as the respective central transitions (CTs, with $k = 0$). Satellite transitions (STs), when present, have a much stronger orientation dependence, with their intensities spread out over a range of frequencies, and hence show lower intensity. The spectra are consistent with a single crystallographic site for ^{51}V and ^{45}Sc, as is expected from the crystal structure. Both nitrides crystallize in the rock-salt structure type, with space group $Fm\bar{3}m$ (no. 225).[28,29]

The MAS spectra confirm that no significant quadrupolar coupling interaction occurs for the studied nuclides, as

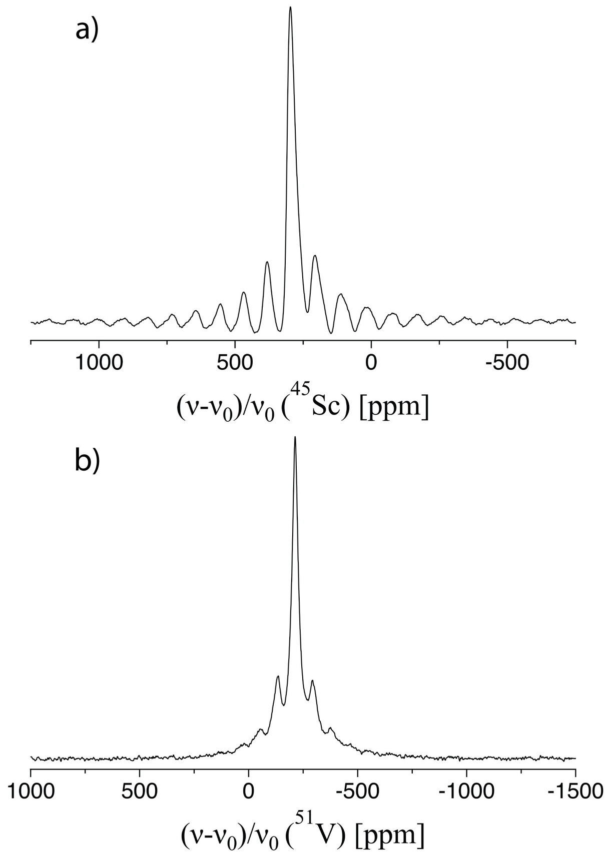

Figure 1. MAS spectra at 10 kHz spinning speed for the polycrystalline ScN- and VN-samples with a) the ^{45}Sc-NMR measurement and b) ^{51}V showing the corresponding center-bands at 290 ppm and at −213 ppm.

expected for these highly symmetric compounds. This conclusion can be drawn from the fact that both central transitions have no characteristic lineshape, but are present as single, symmetrical signals. With sufficiently large quadrupolar coupling, such a special appearance would be observable, because the CT is influenced by second-order effects, containing terms scaling with $\cos^4(\theta)$ which cannot be averaged out by MAS.

The ^{45}ScN spectrum, however, shows an appreciable spinning sideband (SSB) pattern, indicating the presence of anisotropic interactions, which in contrast to the dipolar couplings (see above) are not fully averaged by MAS. These interactions could be either chemical shift anisotropy (CSA) or quadrupolar coupling, the latter introduced by small deviations from ideal symmetry. There could also be a distribution of either interaction, since it is known that achieving an exact stoichiometric ratio for ScN is a challenging task. The kinetics of the direct reaction of Sc metal with nitrogen gas are slow, which may result in nitrogen-deficient products.[30] Also, for the synthesis from the elements, impurities by O-atoms are not improbable. This is due to the high affinity of scandium metal to oxygen[31] and, in comparison with thin films of TiN or ZrN, also of scandium nitride[32] to oxygen. The problem of vacancy formation for the cation sites has also been studied theoretically.[33] The presence of even small concentrations of vacancies or oxygen at anion sites causes distortions of the highly symmetric structure, leading to anisotropies which we observe as a SSB pattern in the NMR spectrum. Moreover, vacancy formation as a random process is likely to introduce a distribution of distortions, leading to additional line broadening. This results in a general broadening of the ^{45}Sc resonances, as observed in Figure 1a in comparison to the ^{51}V spectrum in Figure 1b, with the same difference in broadening being observed in the ^{14}N spectra (see below). While instances of ^{45}Sc CT spectra which are dominated by the CSA instead of the quadrupolar interaction have been reported,[34] the quadrupolar interaction is the more likely source for the anisotropies observed in the NMR spectra here. It should be clearly stated, however, that the experimental evidence does not allow us to distinguish between these interactions, so either or both could be the cause.

It is important to ask whether the position of the strong central resonance in Figure 1a is also affected by the quadrupolar interaction, which would have to be taken into consideration when determining the isotropic shift. To estimate that effect, we assume the quadrupolar interaction to be the main source of the anisotropy. Then, an upper limit for the quadrupolar coupling constant C_q can be derived from the extent of the SSB pattern. For this, the satellite transitions are considered to be affected only by the first-order contribution, since the quadrupolar coupling, if present at all, must be comparatively small. Also, the ^{45}Sc atoms reside on three-fold rotation axes (Wyckoff position 4*b* in the crystal structure), so the EFG tensor is uniaxial with an asymmetry parameter of $\eta = 0$. In this case, the relevant equation in *k*-notation is:[24,25]

$$\nu_Q^{(1)}(k) = -k \cdot \frac{3C_q}{2I(2I-1)} \cdot \frac{(3\cos^2\beta - 1)}{2} \tag{3}$$

The maximum extent is expected for the satellite transitions with $k = \pm 3$, and an angle of $\beta = 0^\circ$ to the external magnetic field. This amounts to approximately 120 kHz, as can be measured from the spectrum in Figure 1a. From this value, an upper limit of $C_q^{\max} = (14 \cdot 120\ \text{kHz})/3 = 560$ kHz can be calculated using Equation (3). In principle, the presence of a sizeable quadrupolar interaction may also affect the resonance position of the central transition via the quadrupolar-induced shift (QIS), which (for $\eta = 0$ and $I = 7/2$) is given by:[35]

$$\nu_{\text{QIS}}^{(2)} = -\frac{1}{392} \cdot \frac{(C_q)^2}{\nu_0} \tag{4}$$

With the relevant values for our ^{45}Sc spectrum, Equation (4) returns 6.58 Hz, or 0.05 ppm, which obviously may be safely ignored. Therefore, the position of 290 ppm can be identified as being the isotropic chemical shift of ^{45}Sc in ScN.

It may be seen from Figure 1b that the SSB pattern of the ^{51}V spectrum of VN is only a fraction of the width of that of the ^{45}Sc spectrum of ScN. Hence, without repeating the above discussion about ^{45}Sc, it can also be concluded for ^{51}V that the observed resonance frequency of −213 ppm corresponds to the isotropic chemical shift. Although negative, this shift value is well within the range commonly observed for diamagnetic vanadium compounds.[36]

NMR of spin-1: ^{14}N

The MAS spectra of Sc^{14}N and V^{14}N are shown in Figure 2. The ^{14}N nucleus has spin $I = 1$, and a comparatively large quadrupole moment. Thus, even for small distortions of the electronic environment,[37] the separation of the two transitions $k = \pm 1/2$ becomes visible, leading to a symmetric doublet in the static NMR spectrum. For many nitrogen-containing compounds, these doublets are very broad, requiring specialized wide-line techniques for spectra acquisition.[38] This doublet lineshape also persists in the appearance of the sidebands under MAS conditions, even for quadrupolar coupling constants of only about 140 kHz, such as for *h*-B^{14}N.[39] In principle, however, MAS is capable of fully averaging the effects caused by quadrupolar coupling to first order, with the efficiency of averaging determined by the ratio of coupling constant to MAS rate. While the spectra of VN and ScN in Figure 2 show a single high-intensity resonance, spinning sidebands (SSB) are also clearly present in the ^{14}N spectra. Again, experimental evidence does not allow us to distinguish between CSA and quadrupolar coupling as the source of the anisotropy manifested by the presence of the SSBs. Assuming quadrupolar interaction to be the main source, an upper limit for C_q may be derived by comparing the spectra in Figure 2 to computer simulations. Using the SIMPSON package,[40] we compared the ratio of the SSB intensities relative to the main resonance. The experimental

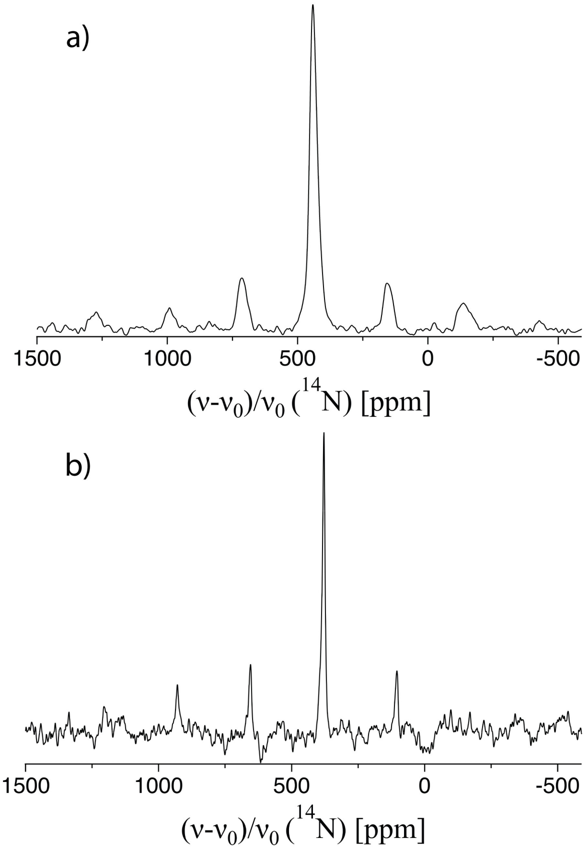

Figure 2. ^{14}N-NMR MAS spectra at 10 kHz spinning speed for a) the polycrystalline ScN and b) the VN sample with the center bands appearing at 442 ppm and 378 ppm, respectively.

intensities are consistent with a $C_q < 25$ kHz, with coupling constants above that resulting in significantly higher SSBs. Irrespective of the cause of the SSB pattern, the isotropic chemical shift may be obtained directly from the resonance positions for both nitrides.

Relation of ^{14}N chemical shift to crystal structure

For the application of solid-state NMR spectroscopy as an analytical tool, there is always interest in correlating NMR parameters to structural features, e.g. distances or angles.[20]

One example is to plot the values of the isotropic chemical shift, δ_{iso}, against the mean distance to the next atoms constituting the coordination sphere and postulating a linear dependence between these two parameters. This has been demonstrated for compounds with PbO_x,[41] NaO_x,[42] or AlO_x[20] polyhedra. Since the specification of a coordination sphere is neither unique nor simple even with the inclusion of complex calculations,[43] it has been suggested to use the shortest X–O distance instead.[44] The shortest distance is not only uniquely defined, but is also an indirect measure of the average distance to the next neighbouring atoms in the structure. In an attempt to apply this concept to nitrogen chemical shifts, the δ_{iso} values for ^{14}N for the binary nitrides listed in Table 1 were plotted against the shortest distance to the nearest cation, as taken from the XRD structure determinations. This resulted in a comparatively good linear correlation with a Pearson correlation coefficient *R* of 0.88, as may be seen from Figure 3. It should be noted, however, that a clear theoretical foundation for this linear relation does not exist.

Conclusions

The binary nitrides ScN and VN have been characterized by ^{45}Sc-, ^{51}V- and ^{14}N-NMR. For all nuclides, the effects of quadrupolar interaction are small, leading to narrow lines in the MAS spectra, which are comparatively easy to detect even for modest sample amounts. The results presented here may also be useful for identifying these nitrides in multi-phase samples. Regarding general aspects of nitrogen NMR of binary nitrides, it

Table 1. Determined ^{14}N isotropic chemical shifts for the investigated and selected binary nitrides, listed in ascending order (values referenced against solid NH_4Cl).

Compound	Structure Type	Isotropic Shift
c-BN	Sphalerite[45]	−17.6 ppm[39]
h-BN	Graphite-like[46]	61.2 ppm[39]
AlN[a]	Wurtzite[47]	62.4 ppm[48]
GaN[a]	Wurtzite[49]	270.4 ppm[50]
InN[a]	Wurtzite[51]	270.9 ppm[50]
TiN	Rock-salt[52]	359 ppm[37]
ZrN[a]	Rock-salt[53]	361.4 ppm[50]
VN	Rock-salt[28]	378 ppm
ScN	Rock-salt[29]	442 ppm

[a] values for δ_{iso} re-referenced against NH_4^+

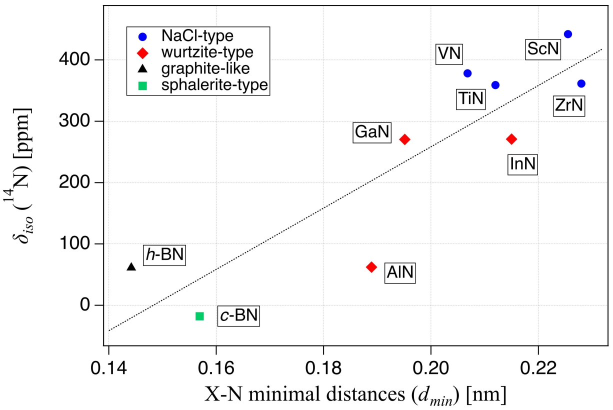

Figure 3. Plot of nitrogen isotropic chemical shift values (determined via ^{14}N-NMR) versus the shortest X–N distance in each crystal structure (with the data given by Table 1). The line corresponds to a linear fit according to the expression
δ_{iso} (^{14}N)[ppm] $= a + b \cdot d_{min}$ [nm]. The obtained fit parameters with their respective errors were: $a = -740 \pm 200$, $b = 4993 \pm 1010$ and the correlation coefficient $R = 0.88$.

could be shown that the isotropic chemical shift relates to the distance of the nearest nitrogen to the respective cation.

In general, research and development involving nitride compounds is still a vibrant field, as partly reviewed in the Introduction of this paper. In particular, the group of *Wolfgang Schnick* has been very productive in this field of research over the last decades.[15,16,54–56]

Experimental Section

The investigated scandium nitride has been synthesized from the elements as described by *Niewa et al.*[30] Vanadium nitride has also been prepared according to literature.[57] Phase purity was confirmed by powder X-Ray diffraction for both nitrides.

Polycrystalline samples of the compounds were filled into a 4 mm rotor and spun at a frequency of 10 kHz. The single-pulse MAS-measurements were carried out on a Bruker Avance-III 500 spectrometer at LMU Munich with the corresponding Larmor frequencies being $\nu_0(^{14}\mathrm{N}) = 36.141$ MHz, $\nu_0(^{45}\mathrm{Sc}) = 121.490$ MHz and $\nu_0(^{51}\mathrm{V}) = 131.549$ MHz. A baseline correction was applied for both ^{14}N experiments and for the Sc^{14}N-data, an additional two point left shift in order to reduce ringdown effects. The line broadening applied for all spectra in this work is 500 Hz, except for the V^{14}N with 200 Hz. Furthermore, recycle delays of 0.5 s and 80 scans for ^{51}VN, 20 s and 4096 scans for V^{14}N, 64 s and 24 scans for ^{45}ScN as well as 60 s and 100 scans for Sc^{14}N were used. ^{14}N spectra were referenced against solid NH_4Cl, ^{45}Sc against an aqueous solution of $ScCl_3$, and ^{51}V against the secondary reference of the ^{1}H resonance of 1% $Si(CH_3)_4$ in $CDCl_3$, all set to 0 ppm.

For the syntheses of vanadium nitride achieving full stoichiometry may be difficult. A thermodynamically favourable vacancy formation enthalpy even stabilizes the NaCl-structure for VN_x-samples[58] (with $x < 1$) for which a strong paramagnetism is observable.[59] Furthermore, a high electrical conductivity has been determined of about 1.6×10^6 S/m[10] and it was also published that properties like the magnetic susceptibility or superconducting transition temperature depend on the V:N-ratio.[60] Therefore, it was necessary to dilute the sample in the rotor with a non-nitrogen containing compound (ZrO_2) to achieve stable spinning. Similar problems were already encountered for the electrically conductive transition metal nitride TiN.[37,61]

Acknowledgements

Open Access funding enabled and organized by Projekt DEAL.

Data Availability Statement

The data that support the findings of this study are available from the corresponding author upon reasonable request.

Conflict of Interest

The authors declare no conflict of interest.

Keywords: binary nitrides · ^{51}V^{14}N · ^{45}Sc^{14}N · MAS-NMR · isotropic chemical shifts

[1] Y. Taniyasu, M. Kasu, T. Makimoto, *Nature* **2006**, *441*, 325–328.
[2] S. Marauska, T. Dankwort, H. J. Quenzer, B. Wagner, *Procedia Eng.* **2011**, *25*, 1341–1344.
[3] T. Polster, M. Hoffmann, *Procedia Chem.* **2009**, *1*, 144–147.
[4] T. K. Harris, E. J. Brookes, C. J. Taylor, *Int. J. Refract. Met. Hard Mater.* **2004**, *22*, 105–110.
[5] J. He, J. Sun, Y. Meng, X. Yan, *Surf. Topogr.: Metrol. Prop.* **2019**, *7*, 015022.
[6] F. Hui, C. Pan, Y. Shi, Y. Ji, E. Grustan-Gutierrez, M. Lanza, *Microelectron. Eng.* **2016**, *163*, 119–133.
[7] E. Santecchia, A. M. S. Hamouda, F. Musharavati, E. Zalnezhad, M. Cabibbo, S. Spigarelli, *Ceram. Int.* **2015**, *41*, 10349–10379.
[8] H. Kuwahara, N. Mazaki, M. Takahashi, T. Watanabe, X. Yang, T. Aizawa, *Mater. Sci. Eng. A* **2001**, *319–321*, 687–691.
[9] L. P. B. Lima, J. A. Diniz, I. Doi, J. G. Fo, *Microelectron. Eng.* **2012**, *92*, 86–90.
[10] Y. Liu, Q. Wu, L. Liu, P. Manasa, L. Kang, F. Ran, *J. Mater. Chem. A* **2020**, *8*, 8218–8233.
[11] X.-P. Qu, M. Zhou, T. Chen, Q. Xie, G.-P. Ru, B.-Z. Li, *Microelectron. Eng.* **2006**, *83*, 236–240.
[12] N. Tureson, N. V. Nong, D. Fournier, N. Singh, S. Acharya, S. Schmidt, L. Belliard, A. Soni, A. le Febvrier, P. Eklund, *J. Appl. Phys.* **2017**, *122*, 025116.
[13] H. Yang, S. Heo, D. Lee, S. Choi, H. Hwang, *Jpn. J. Appl. Phys.* **2006**, *45*, L83.
[14] K. H. Jack, *J. Mater. Sci.* **1976**, *11*, 1135–1158.
[15] L. Eisenburger, V. Weippert, O. Oeckler, W. Schnick, *Chem. Eur. J.* **2021**, *27*, 14184–14188.
[16] L. Eisenburger, V. Weippert, C. Paulmann, D. Johrendt, O. Oeckler, W. Schnick, *Angew. Chem.* **2022**, *134*, 1–5; *Angew. Chem. Int. Ed.* **2022**, *61*, 1–5.
[17] V. S. Bhadram, D. Y. Kim, T. A. Strobel, *Chem. Mater.* **2016**, *28*, 1616–1620.
[18] V. S. Bhadram, H. Liu, E. Xu, T. Li, V. B. Prakapenka, R. Hrubiak, S. Lany, T. A. Strobel, *Phys. Rev. Mater.* **2018**, *2*, 011602.
[19] H. O. Pierson, in *Handbook of Refractory Carbides and Nitrides*, Elsevier, **1996**, pp. 156–162.
[20] K. J. D. MacKenzie, M. E. Smith, in *Multinuclear Solid-State NMR of Inorganic Materials*, Pergamon Press, Oxford, **2002**.
[21] T. Bräuniger, M. Jansen, *Z. Anorg. Allg. Chem.* **2013**, *639*, 857–879.
[22] R. Dupree, M. H. Lewis, M. E. Smith, *J. Appl. Crystallogr.* **1988**, *21*,109–116.
[23] T. Bräuniger, P. Kempgens, R. K. Harris, A. P. Howes, K. Liddell, D. P. Thompson, *Solid State Nucl. Magn. Reson.* **2003**, *23*, 62–76.
[24] M. H. Cohen, F. Reif, *Solid State Phys.* **1957**, *5*, 321–438.
[25] O. E. O. Zeman, T. Bräuniger, *Solid State Nucl. Magn. Reson.* **2022**, *117*, 101775.
[26] M. H. Levitt, in *Spin Dynamics: Basics of Nuclear Magnetic Resonance, 2nd ed.*, John Wiley & Sons Ltd., Chichester, **2008**, pp. 211–217.
[27] E. R. Andrew, *Philos. Trans. R. Soc. London Ser. A* **1981**, *299*, 505–520.
[28] M. Hasegawa, T. Yagi, *J. Alloys Compd.* **2005**, *403*, 131–142.
[29] H. P. Klesnar, P. Rogl, *High Temp. High Pressures* **1990**, *22*, 453–457.
[30] R. Niewa, D. A. Zherebtsov, M. Kirchner, M. Schmidt, W. Schnelle, *Chem. Mater.* **2004**, *16*, 5445–5451.
[31] R. Deng, F. Liu, L. Tan, S. Zhang, Y. Liu, L. Huang, *J. Alloys Compd.* **2019**, *785*, 634–641.
[32] M. A. Moram, Z. H. Barber, C. J. Humphreys, *Thin Solid Films* **2008**, *516*, 8569–8572.

[33] J. Missaoui, I. Hamdi, N. Meskini, *J. Magn. Magn. Mater.* **2016**, *413*, 19–24.
[34] T. Bräuniger, P. Bielec, O. E. O. Zeman, I. L. Moudrakovski, C. Hoch, W. Schnick, *Z. Naturforsch. B* **2021**, *76*, 217–225.
[35] E. Kundla, A. Samoson, E. Lippmaa, *Chem. Phys. Lett.* **1981**, *83*, 229–232.
[36] O. B. Lapina, D. F. Khabibulin, A. A. Shubin, V. V. Terskikh, *Prog. Nucl. Magn. Reson. Spectrosc.* **2008**, *53*, 128–191.
[37] T. Bräuniger, T. Müller, A. Pampel, H.-P. Abicht, *Chem. Mater.* **2005**, *17*, 4114–4117.
[38] L. A. O'Dell, *Prog. Nucl. Magn. Reson. Spectrosc.* **2011**, *59*, 295–318.
[39] G. Jeschke, W. Hoffbauer, M. Jansen, *Solid State Nucl. Magn. Reson.* **1998**, *12*, 1–7.
[40] M. Bak, J. T. Rasmussen, N. C. Nielsen, *J. Magn. Reson.* **2000**, *147*, 296–330.
[41] F. Fayon, I. Farnan, C. Bessada, J. Coutures, D. Massiot, J. P. Coutures, *J. Am. Chem. Soc.* **1997**, *119*, 6837–6843.
[42] A. M. George, S. Sen, J. F. Stebbins, *Solid State Nucl. Magn. Reson.* **1997**, *10*, 9–17.
[43] R. Hoppe, *Z. Kristallogr.* **1979**, *150*, 23–52.
[44] O. E. O. Zeman, J. Steinadler, R. Hochleitner, T. Bräuniger, *Crystals* **2019**, *9*, 43.
[45] V. Kupcik, J. Grochowski, P. Serda, *Z. Kristallogr.* **1994**, *209*, 236–238.
[46] E. Budak, C. Bozkurt, *Physica B* **2010**, *405*, 4702–4705.
[47] H. Schulz, K. H. Thiemann, *Solid State Commun.* **1977**, *23*, 815–819.
[48] O. E. O. Zeman, I. L. Moudrakovski, C. Hartmann, S. Indris, T. Bräuniger, *Molecules* **2020**, *25*, 469.
[49] V. Petkov, M. Gateshki, J. Choi, E. G. Gillan, Y. Ren, *J. Mater. Chem.* **2005**, *15*, 4654–4659.
[50] P. Kempgens, J. Britton, *Magn. Reson. Chem.* **2015**, *54*, 371–376.
[51] W. Paszkowicz, R. Černý, S. Krukowski, *Powder Diffr.* **2003**, *18*, 114–121.
[52] C.-C. Jiang, T. Goto, T. Hirai, *J. Alloys Compd.* **1993**, *190*, 197–200.
[53] M. Yang, J. A. Rodgers, L. C. Middler, J. Oró-Solé, A. B. Jorge, A. Fuertes, J. P. Attfield, *Inorg. Chem.* **2009**, *48*, 11498–11500.
[54] J. Häusler, W. Schnick, *Chem. Eur. J.* **2018**, *24*, 11864–11879.
[55] S. B. Schneider, D. Baumann, A. Salamat, W. Schnick, *J. Appl. Phys.* **2012**, *111*, 093503.
[56] W. Schnick, *Angew. Chem.* **1999**, *111*, 3511–3512; *Angew. Chem. Int. Ed.* **1999**, *38*, 3309–3310.
[57] M. Qin, H. Wu, Z. Cao, D. Zhang, B. Jia, X. Qu, *J. Alloys Compd.* **2019**, *772*, 808–813.
[58] C. Ravi, H. K. Sahu, M. C. Valsakumar, A. van de Walle, *Phys. Rev. B* **2010**, *81*, 104111.
[59] B. R. Zhao, L. Chen, H. L. Luo, *Phys. Rev. B* **1984**, *29*, 6198–6202.
[60] F. I. Ajami, R. K. MacCrone, *J. Phys. Chem. Solids* **1975**, *36*, 7–15.
[61] K. J. D. MacKenzie, R. H. Meinhold, D. G. McGavin, J. A. Ripmeester, I. Moudrakovski, *Solid State Nucl. Magn. Reson.* **1995**, *4*, 193–201.

Manuscript received: June 14, 2022
Revised manuscript received: September 21, 2022